Surface behavior of sphingomyelins with very long chain polyunsaturated fatty acids and effects of their conversion to ceramides

Journal:	*Langmuir*
Manuscript ID:	la-2014-00485x.R1
Manuscript Type:	Article
Date Submitted by the Author:	n/a
Complete List of Authors:	Peñalva, Daniel; Instituto de Investigaciones Bioquímicas de Bahía Blanca (INIBIBB), Universidad Nacional del Sur and Consejo Nacional de Investigaciones Científicas y Técnicas (CONICET) Wilke, Natalia; Universidad Nacional de Córdoba, Departamento de Química Biológica Maggio, Bruno; Centro de Investigaciones en Química Biológica de Córdoba (CIQUIBIC, UNC–CONICET), Departamento de Química Biológica,, Aveldaño, Marta; Bahía Blanca Institute for Biochemical Research, Fanani, Maria; Universidad Nacional de Cordoba- CONICET, Quimica Biologica- CIQUIBIC

Surface behavior of sphingomyelins with very long chain polyunsaturated fatty acids and effects of their conversion to ceramides

Daniel A. Peñalva[1]., Natalia Wilke[2], Bruno Maggio[2]., Marta I. Aveldaño[1]., Maria L. Fanani[2]*

1. Instituto de Investigaciones Bioquímicas de Bahía Blanca (INIBIBB), Universidad Nacional del Sur and Consejo Nacional de Investigaciones Científicas y Técnicas (CONICET), 8000 Bahía Blanca, Argentina.

2. Departamento de Química Biológica, Centro de Investigaciones en Química Biológica de Córdoba (CIQUIBIC), Facultad de Ciencias Químicas, Universidad Nacional de Córdoba and CONICET, 5000 Córdoba, Argentina.

** to whom correspondence should be addressed. E-mail: lfanani@fcq.unc.edu.ar*

Short title:

Films of sphingomyelins and ceramides with very-long-chain fatty acids

ABSTRACT

Molecular species of sphingomyelin (SM) with nonhydroxy (n) and 2-hydroxy (h) very-long-chain polyunsaturated fatty acids (n- and h-28:4, 30:5 and 32:5) abound in rat spermatogenic cells and spermatozoa. These SMs are located on the sperm head, where they are converted into the corresponding ceramides (Cer) after completion of the acrosomal reaction, as induced in vitro. The aim of this study was to look into the surface properties of these unique SM species and how these properties change by the SM→Cer conversion. After isolation by HPLC, these SMs were organized in Langmuir films and studied alone, in combination with different proportions of Cer, and during their conversion into Cer by sphingomyelinase. Compression isotherms for all six SMs under study were compatible with a liquid-expanded (LE) state and showed large molecular areas. Only the longest SMs (n-32:5 and h-32:5 SM) underwent a phase transition upon cooling. On the other hand, the abundant h-28:4 Cer exhibited an unusual highly compressible liquid-condensed (LC) phase, compatible with a high conformational freedom of Cer molecules but with the characteristic low diffusional properties of the LC phase. In mixed films of h-28:4 SM / h-28:4 Cer, the components showed a favourable mixing in the LE phase. The monolayer exhibited h-28:4 Cer-rich domains both in premixed films and when formed by the action of sphingomyelinase on pure h-28:4 SM films. In conclusion, while the SMs from sperm behaved in a way similar to shorter acylated SMs, the corresponding Cers showed atypical rheological properties that may be relevant for the membrane structural rearrangements that take place on the sperm head after completion of the acrosomal reaction.

Supplementary key words: 2-hydroxy fatty acids; Brewster angle microscopy; single particle tracking; Langmuir monolayers; two-dimensional phase transitions; liquid-condensed domains.

1. INTRODUCTION

In mammalian spermatozoa, sphingomyelin (SM) is made up of molecular species that contain very-long-chain (C24 to C34) polyunsaturated fatty acids (VLCPUFA) N-linked to sphingosine.[1-3] These fatty acids, in proportions that vary among species, are elongated versions of common PUFA of the n-6 series (like arachidonic or docosapentaenoic acids) or the n-3 series (like eicosapentaenoic or docosahexaenoic acids). In some mammals including the rat, part of the VLCPUFA of sperm SM are 2-hydroxylated.[4]

In the rat, nonhydroxy VLCPUFA (n-V) and 2-hydroxy VLCPUFA (h-V) also occur in the ceramide (Cer) fraction of testicular spermatogenic cells and of mature gametes.[5] The small head of rat sperm contains n-V SM or h-V SM as predominant SM species but no Cer, which instead is present in the large sperm tail in the form of h-V Cer species.[6]

In rat sperm, membrane glycerophospholipids and SM undergo a series of hydrolytic changes after undergoing sperm-specific physiological changes, as capacitation and completion of the acrosomal reaction.[7] The enzymatically driven SM → Cer conversion leads to gametes that are relatively enriched in n-V Cer and h-V Cer species.[7] Based on previous studies on different species of SM being converted to Cer by the action of sphingomyelinase (SMase),[8-10] such an increase of the Cer / SM mole ratio may be envisaged to have an important impact on the sperm surface properties.[11,12] However, the biophysical properties and behavior of VLCPUFA-containing SM and Cer are just beginning to be understood.

In a previous study, the SM species containing the six fatty acids represented in Fig. 1 (n- and h-) 28:4 n-6, 30:5 n-6 and 32:5 n-6, were analyzed using fluorescence approaches in bilayer systems, in pure form and in mixtures with a typical glicerophospholipid like phosphatidylcholine (PC) and with cholesterol (Chol).[13] Only the longest n-32:5 SM and h-32:5 SM displayed a gel-liquid transition temperature (Tm ≈ 21–22°C), the rest remaining in the liquid state over the 5°C–45°C range. The degree of order was lower in bilayers of any of the n-V SMs than in those of their chain-matched h-V SMs. Both, but n-V SM relatively more than h-V SM, decreased the Tm of dimyristoyl-PC as their proportion increased in binary PC:SM liposomes. In contrast to the established ability of 16:0 SM to form lateral SM/Chol domains in dioleoylPC:Chol:SM bilayers,[14-16] these domains were not formed when the SM had VLCPUFA.

Regarding the SM-related Cer molecules, when compared to the more ubiquitous molecular species of Cer previously described in the literature,[17-19] the (n- and h-) 28:4, 30:5 and 32:5 Cer species also behaved atypically, as reported in a recent study using Langmuir monolayers.[20] Surface pressure and surface potential measurements, and imaging by Brewster angle microscopy (BAM) were used to understand their average molecular organization at the air-liquid interface. Although differences were observed between n-V Cer and h-V Cer (for example, a closer molecular packing in the latter than in the former at a given pressure, ascribable to the 2-hydoxyl group), all of them revealed much larger mean molecular areas (MMA) and molecular dipole moments in liquid expanded (LE) phases than 16:0 Cer or 24:1 Cer. In addition, all VLCPUFA-Cer

showed LE to liquid-condensed (LC) transitions with domain segregation at room temperature, as confirmed by BAM.

The aim of the present study was to look into the surface properties of Langmuir films composed by the n-V SM and h-V SM species that have the same N-linked acyl chains as the previously studied Cers (Fig. 1), both when they are in pure form and when they are in the presence of varying proportions of the corresponding Cer. Keeping in mind that the SM → Cer conversion is one of the irreversible changes that affect the sperm lipid in the environment of an oocyte ready to be fertilized, mixtures of h-28:4 SM and h-28:4 Cer in various proportions, or dynamically generated by employing h-28:4 SM as substrate of SMase, were used as models. Our results showed that, while the SMs from sperm behave in a way that is similar to that of other SMs, which would be compatible with a stable LE planar membrane structure at nearly physiological temperatures, the corresponding Cer showed atypical rheological properties. The present study might contribute to understand structural changes taking place in the sperm membrane before fertilization.

2. MATERIALS AND METHODS

2.1. Sphingomyelins and ceramides: 16:0 SM, 18:1 SM, 16:0 Cer and 18:1 Cer were from Avanti Polar Lipids Co (Alabaster, AL). The SM and Cer species with n- and h-very long chain PUFA were obtained from adult Wistar rat testes using a combination of TLC and HPLC procedures.[13,20]

2.2. Monolayer compression isotherms: Langmuir Isotherms were obtained with a KSV Minitrough equipment (KSV, Helsinski, Finland) equipped with a Pt plate for measuring the surface pressure.[21] In some experiments the surface potential of the film was simultaneously measured with a surface ionizing electrode formed by a ^{241}Am plate positioned 5 mm above the monolayer surface, and a reference Ag / $AgCl_2$ (3M) electrode connected to the aqueous subphase. The whole system was enclosed in an acrylic box, saturated with N_2 gas to prevent lipid peroxidation, and surrounded by a metallic grid connected to ground to reduce external interference in surface potential measurements. Experiments were performed using a subphase of 145 mMNaCl kept at 22°C or 7°C (± 1°C) by means of an external circulating water bath (Haake F3C). Absence of surface active impurities in the subphase solutions or in the spreading solvents was checked routinely. Lipid monolayers were obtained by spreading adequate aliquots of chloroformic solutions of SM, Cer or SM / Cer onto the aqueous surface. After allowing 5 min for solvent evaporation, surface pressure-area isotherms were recorded while compressing the monolayers at a constant rate of 2 $Å^2$. $molecule^{-1}.min^{-1}$. The compressibility modulus (C_s^{-1})[22] was calculated from the isotherm data as:

$$Cs^{-1} = -MMA\left(\frac{\partial \pi}{\partial MMA}\right)_T \quad \text{(Eq. 1)},$$

where MMA is the mean molecular area at a given surface pressure (π). The resultant dipole moment perpendicular to the interface ($\mu_\perp$)[22] of Cer at each molecular area was calculated from surface potential and isotherm data as:

$$\mu_{\perp} = \frac{1}{12\pi} MMA\Delta V \quad \text{(Eq. 2)},$$

where ΔV is the surface potential of the monolayer at the corresponding MMA, and π in this case is the mathematical Euclidean constant taken as 3.1416. The intermolecular interaction of SM molecules in a LE monolayer was evaluated using the following expression:

$$(\pi - \pi_s)\,(MMA - A_0) = kT \quad \text{(Eq. 3)},$$

where π_s is the interaction pressure, A_0 is the molecular limiting area[23] and *k* is the Boltzmann constant. This model describes the behavior of LE films assuming a constant cohesion between the lipid molecules as they are compressed, which was applied satisfactorily to compression curves under 20mN/m (R^2>0.94).

2.3. Effects of SMase activity on Langmuir monolayers: SM monolayers were formed at the surface of an all-Teflon zero-order trough, under stirring. *Bacillus cereus* SMase (final concentration, 1.68 mU/ml) was injected into the buffered subphase (10 mM Tris/HCl, 125 mM NaCl, 3mM MgCl, pH 8) for conversion of SM into Cer and phosphorylcholine. While the latter solubilizes into the subphase, Cer remains at the interface. Due to the difference in cross-sectional area between SM and Cer, the reaction progress can be followed in real time by the reduction of the total monolayer area.[8,24] A reservoir compartment adjacent to the reaction compartment and connected by a narrow and shallow slit served as substrate monolayer reservoir (pure SM). As the reaction took place, the total monolayer area was automatically compensated in order to keep the surface pressure constant through the movement of a barrier in the reservoir compartment, which allowed keeping a constant area on the reaction compartment during the SM → Cer conversion.

2.4. Diffusion coefficient of micro-spheres on SM and Cer monolayers: Latex beads of 3 µm diameter (LB30, Sigma) were centrifuged and washed 6-times with clean water. 5 µL of the aqueous suspension of beads was added to 100µL of the ~~lipid~~ SM solutions (solvent, chloroform:methanol, 2:1, by vol), immediately before spreading onto the air/NaCl solution interface. After monolayer compression, the movement of the beads on the surface of the different species was followed by phase contrast microscopy at a rate of 14 frames per second. The position of beads in each frame was tracked using the plug-in software "Tracker_classof" associated to the ImageJ 1.43u programme (NIH, USA). The mean square displacement of a single latex bead particle relative to another one in the same frame (MSD) was calculated. Determination of the relative bead positions minimizes the effect of the drift (always present in Langmuir monolayers) on the calculation of the Brownian motion and the diffusion coefficient (D) can be obtained from:

$$MSD = 8D.\delta t \quad \text{(Eq. 4)},$$

where δt is the time interval analyzed.[25]

2.5. Brewster angle microscopy: BAM visualization was performed with an auto-nulling imaging ellipsometer (Nanofilm EP3sw imaging ellipsometer, Accurion GmbH,

Germany) working in the BAM mode. The minimum of the reflection was set with a polarized 532 nm laser incident on the bare aqueous surface and set at the experimentally calibrated Brewster angle (53.1°). After monolayer formation and compression, the reflected light was collected with a 20 X objective and a CCD camera, which operates at a resolution of 1μm. For a better visualization, the lower 0-100 gray level range (from the 0-255 original scale) was selected in BAM images. BAM observation of SM monolayers treated with SMase was performed as follows: The subphase volume of the rectangular compartment was restricted with a cylindrical glass ring connected by a surface slit of etched glass with the rest of the surface of the trough. The lipid monolayers were spread on the aqueous surface and compressed to the desired pressure. The solution containing SMase was injected in the subphase, within the glass encircled compartment, and the reflected light was collected as a function of time. The gray level of BAM pictures depends on the thickness and refraction index of the film,[17,26] then LC domains, which are usually thicker and show higher refraction index than the LE phase, appear as light gray areas surrounded by a dark gray LE phase.

3. RESULTS AND DISCUSSION

3.1. Langmuir monolayers of VLCPUFA-containing SM species. The six SM species that contain VLCPUFA examined in this work (Fig. 1) were studied by compression isotherms of monolayers formed on a subphase of NaCl (145 mM). All of them showed a smooth behavior, compatible with a fully liquid expanded (LE) character and collapse pressures in the 40-47 mN/m range (Fig. 2).

This general behavior was similar to that observed with oleoyl SM (18:1 SM). The saturated acyl-chained palmitoyl SM (16:0 SM), used as comparison, showed a phase transition from a LE to liquid-condensed (LC) state at ~22 mN/m and at room temperature, as evidenced by a plateau in the plot relating meanmolecular area (MMA) and surface pressure (π) (Fig. 2).

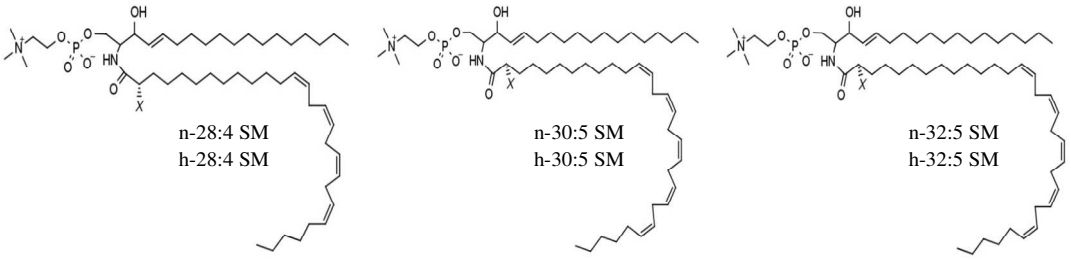

Fig 1.Chemical structures of the sphingomyelin (SM) species than contain N-linked very-long-chain polyunsaturated fatty acids (VLCPUFA) studied in this work. The n- and h- prefixes are used to denote the presence of –H or –OH at the 2-position of the fatty acid, here marked with the X, in nonhydroxy (n) and 2-hydroxy (h) VLCPUFA (V). In the text, these two groups of SM species are abbreviated as n-V SM and h-V SM, respectively. The structures are shown only for illustrative purposes and are not meant to represent the molecular organization adopted by the chains at the air-liquid interface.

The most notable difference between VLCPUFA-containing SMs and the shorter-chain SMs mentioned before was that the former showed significantly larger MMA. The n-32:5 SM showed the largest area, which doubled the area occupied by 16:0 SM (see Fig. 2 and Table 1). A comparison between n-V SMs and h-V SMs showed smaller molecular areas for the latter (Fig. 2 and Table 1). Since this result was also obtained previously for h-V Cer compared to n-V Cer species,[20] it appears as a general behavior that the presence of the 2-hydroxyl group in the fatty acid favors stronger intermolecular interactions leading to smaller areas. This effect also correlated with previous data in bilayer systems.[13] Thus, in binary vesicles made of these SM and dimyristoyl PC (DMPC), the three h-V SMs increased the degree of order to a larger extent than their chain-matched n-V SMs. These differences may be ascribed to a more compact packing attained by the h-V SMs compared to the n-V SMs.

The compressibility modulus (Cs^{-1}) of the films reflects their surface elasticity, and has been related to the physical state of the monolayer.[23] The Cs^{-1} parameter calculated for all six VLCPUFA SM species of this study, analyzed at 30 mN/m, gave values lower than ⩽100 mN/m (Table 1). These values were in the same range as those obtained for 18:1 SM in the LE state, and lower than those of saturated SM monolayers such as 16:0 SM, which show Cs^{-1} values higher than ⩾150 mN/m in the LE-LC phase transition region.[27]

Interestingly, the longest n-32:5 and h-32:5 SMs showed even lower Cs^{-1} values, which may reflect a larger conformational freedom upon compression. The free energy of compression (ΔG_c) of the lipid film contains thermodynamic information of the compression process (see section S1 in Supplementary Material). The VLCPUFA-containing SMs showed large ΔG_c values compared to the shorter SMs (Table 1). In the compression process, the overall energetic change reflected by the value of ΔG_c is likely to have an important contribution of the long and unsaturated acyl chains to the entropy loss upon compression.

The entropy associated to the change in area of a lipid film upon compression, $\Delta S_{cf,}$ was estimated after Eq. S4 (from 1 to 35 mN/m), This entropic factor may contribute with 0.27-0.42 kcal/mol to ΔG_c (calculated as $-T.\Delta S_{cf}$) to the area change observed in VLCPUFA-containing SMs monolayers. However, VLCPUFA-containing SMs monolayers showed negligible changes of the ΔG_c values upon cooling (from 22 to 7°C) (data not shown). This contrasted with monolayers of VLCPUFA- Cers, which underwent a significant lowering of ΔG_c (up to 34% decrease) upon cooling from 22 to 8°C),[20] Thus, whereas VLCPUFA-containing Cers showed the expected negative total entropy change upon compression (ΔS_c), in VLCPUFA-containing SMs the entropy factor appears not to be a major contributor to ΔG_c.

Both positive and negative values of ΔS_c have been previously reported for other sphingolipids:[28] The simplest sphingolipids, (Cer and galactosyl-Cer, showed negative ΔS_c, while the more complex gangliosides, which contain large and highly hydrated head groups, showed positive values of ΔS_c. These results were explained considering that in sphingolipids with large head groups the increase of freedom due to the released hydration shell of the polar groups may be an important entropy contributor,

opposing the negative entropy change derived from the ordering of the acyl chains upon compression. Our results may also be explained by these opposing factors, since the very small value of ΔS_c obtained for VLCPUFA-containing SMs may represent a balance between ordering of the acyl chains and disordering of the water molecules associated to the phosphocholine group upon compression.

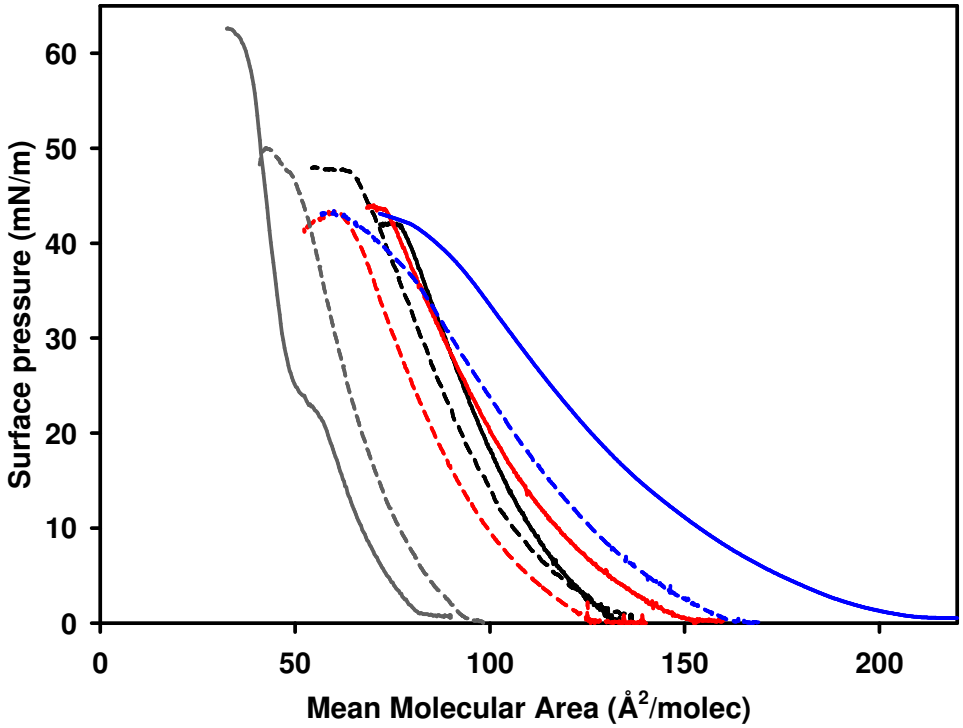

Figure 2.Compression isotherms of SM species with VLCPUFA in monolayers at 22ºC. The solid and dashed lines represent monolayers of n-V SM and h-V SM species, respectively, as follows: n- and h-28:4 SM (black lines), n- and h-30:5 SM (red lines), and n- and h-32:5 SM (blue lines). As a comparison, the isotherms of n-16:0 SM (solid gray line) and of n-18:1 SM (dashed gray line) were also plotted. Each curve shows a representative experiment, differing in less than 2 Å^2/molecule and 2 mN/m from duplicates or triplicates.

Peñalva et al. reported that VLCPUFA-containing ceramides (n-V Cer and h-V Cer) with the same acyl chains as those of the SMs studied here showed MMA values ranging between 58 and 120 Å^2/molecule in the LC phase state and 100–222 Å^2/molecule in the LE phase state, and that the polar headgroup of Cer is small enough to fit under a transverse area section of scarcely 40 Å^2/molecule.[20] This, added to a remarkably high resultant dipole moment perpendicular to the interface ($\mu_\perp$), supported the view that these Cer molecules adopt a bent conformation and partially hydrated acyl chains when organized at the interface. Additionally, and rather unexpectedly, the estimated thickness of the VLCPUFA-containing Cer films was not higher than that of the more common 16:0 Cer.[20]

Because the present SMs have such large acyl chains, the possibility that they organize as rather thick films was investigated. The average volume of an acyl chain has been empirically evaluated in earlier studies for both glycerophospholipids and

sphingolipids[29-31] and it was found to be adequately represented by the following semi-empirical law:

$$V = 2 \times 27.4 + 26.9\,(n_{ch1}+n_{ch2}) \quad \text{(Eq. 5)},$$

where V is the average volume of the hydrocarbon chains and n_{ch1} and n_{ch2} are the number of carbon atoms in each of the hydrocarbon chains. For the SM species with VLCPUFA under study, assuming conservation of the total volume of the hydrocarbon chains, we calculated a semi-empirical thickness (*Th*) as *V*/MMA. This analysis resulted in a *Th* value of 16.2 ± 0.3 Å for 18:1 SM at 30 mN/m.

Unexpectedly, all VLCPUFA-containing SM species except h-30:5 SM showed a *Th* smaller than the latter value (Table 1). Furthermore, the increase in two additional methylene groups between (n- or h-) 30:5 SM and their corresponding homologues, (n- or h-) 32:5 SM, led to even lower values of *Th*,suggesting a thinning of the films. Thus, a longer N-acyl chain would not necessarily imply a thicker monolayer film. Compared to n-V SMs, the presence of the hydroxyl group in the second carbon atom of the fatty acid in the three h-V SMs slightly but consistently tended to increase the semiempirical film thickness.

TABLE 1. Characteristic parameters of monolayers of VLCPUFA-containing SM species and comparison with shorted N-acylated SMs.

Molecular species	MMA[a] (Å^2/molec)	Cs^{-1}[a] (mN/m)	ΔG_c[b] (kcal/mol)	Film thickness[c] *Th* (Å)	Interaction pressure[d], π_s(mN/m)
n-28:4 SM	88 ± 1	94 ± 5	0.51 ± 0.03	14.1 ± 0.2	- 6.1 ± 0.6
n-30:5 SM	88 ± 1	84 ± 6	0.61 ± 0.02	14.7 ± 0.2	- 4.3 ± 0.1
n-32:5 SM	106 ± 1	58 ± 2	1.03 ± 0.02	12.7 ± 0.1	- 1.4 ± 0.1
h-28:4 SM	83 ± 1	90 ± 9	0.57 ± 0.04	14.9 ± 0.2	- 4.8 ± 0.7
h-30:5 SM	75 ± 1	86 ± 5	0.49 ± 0.02	17.2 ± 0.2	- 6.0 ± 0.3
h-32:5 SM	92 ± 1	63 ± 1	0.79 ± 0.01	14.6 ± 0.2	- 3.4 ± 0.1
n-16:0 SM	47 ± 1[e]	160 ± 3	0.35 ± 0.01	19.5 ± 0.4	----------
n-18:1 SM	60 ± 1[e]	106 ± 3	0.36 ± 0.01	16.2 ± 0.3	-8.5 ± 0.4

[a] Taken at 30 mN/m.
[b] Integrating compression isotherms from 1 to 35 mN/m after eq. S1.
[c] Semiempirical film thickness, values calculated as *V*/MMA at 30mN/m.
[d] Calculated after Eq. 3 evaluated on the experimental isotherms under 20mN/m. The non-linear filling resulted in R^2>0.94.
[e] From [27]

With the aim of further evaluating the intermolecular interaction in VLCPUFA-containing SM molecules in the monolayer, Eq. 3 was applied to the compression isotherms to assess the behavior of LE films. Different to gas films, LE films show intermolecular cohesion described as negative values of the interaction pressure parameter (π_s).[23] Compared to 18:1 SM, all VLCPUFA-containing SMs showed less negative values of π_s, which coincided with the semiempirical film thickness (*Th)* tendency. Now,

comparing the three h-V SMs with the corresponding n-V SMs, the former displayed relatively higher interaction pressures (in absolute value) than the latter (Table 1), also in agreement with the *Th* tendency. Since, assuming molecular volume conservation, a thinner film would imply a lower intermolecular Van der Waals attraction, these findings supports the idea that a stronger intermolecular attraction is established when a hydroxyl group is present at the 2C position of the N-acyl chain.

Cooling of VLCPUFA SM monolayers to 7°C induced the formation of an LC phase at high surface pressures only in the case of the longest (h- and n-) 32:5 SM species (Fig. S1). An LE → LC phase transition was observed in the 80-130 $Å^2$/molecule area range, evidenced by a quasi-plateau in the π- MMA and a valley in the Cs^{-1}- MMA plots. Similar to the case of VLCPUFA-Cers[20], this phase transition appeared to be more cooperative for the h-V than for the n-V species, consistent with the proposed stronger intermolecular interaction among species that contain 2-hydroxy fatty acids.

The Brewster angle microscopy (BAM) technique allows imaging of Langmuir films at the air/water interface, the grey level of each region being dependent on the thickness and refraction index of the film.[17] Thus, different phase states are imaged differentially according to their physical properties. As revealed by BAM, the LE → LC phase transition for n-32:5 and h-32:5 SM corresponded to a first order process that involved nucleation and growth of the newly formed LC phase (condensed domains) while immersed in a continuous LE phase (Fig. S1 B). The observation that only these two species, among the six VLCPUFA-SMs studied, displayed a surface pressure-induced LE → LC transition correlated with previous findings on the behavior of the same six VLCPUFA-SMs when organized in bilayer form[13], as these two species were the only ones, , to undergo a temperature induced transition (~21-22°C), the other four remaining in the liquid-disordered state over the 5°C - 45°C range.

3.2. Films containing pure SMs and their comparison with their Cer analogues. In this section we focused our attention on h-28:4 SM, one of the six SM that occur on the rat sperm head, and compared it with h-28:4 Cer and with previously studied Cer and SM containing the saturated 16:0 and the monounsaurated 18:1 acyl chains (for an illustration of the chemical structures see Fig. S2). Monolayers formed by h-28:4 SM displayed a Cs^{-1} value quite similar to that of other SMs in the LE state (Table 2 and [27]). This contrasted with h-28:4 Cer monolayers, which showed a condensed-like phase at high π (30mN/m), as judged from compression isotherms and microscopy data.[20]

The Cs^{-1} value for h-28:4 Cer films (and also for the rest of the VLCPUFA-Cer studied) was low compared to those of 16:0 Cer and 18:1 Cer in condensed/solid states ((Table 2). Considering the usual classification of lipid monolayer states according to the values of Cs^{-1},[23] the low Cs^{-1} values of the h-28:4 Cer film suggests it should be in a LE rather than in a LCstate as it was. This atypical behavior was attributed to the atypical length and polyunsaturation of the acyl chain[20]. In the present work we found that h-28:4 SM behaved similarly to other SMs in the LE state (Table 2) and showed Cs^{-1} values lower than other SMs but somewhat higher than those of h-28:4 Cer, even when the latter is expected to be in an LC state. Thus, a conversion from a h-28:4 SM film in the LE state to a h-28:4 Cer film in the LC state (for instance, under the action of

sphingomyelinase) should be expected to lead to an increase of the Cs^{-1} of the film, i.e., opposite to the observed behavior.

In order to more accurately define the phase state of monolayers for each of these two lipids, the shear viscosity was tested using single particle tracking experiments (Fig. 3). Micrometer-sized latex beads were spread onto SM or Cer monolayers and their diffusion mobility in each film was compared. The dependence of the mean square displacement (MSD) of the beads with the time interval is proportional to the diffusion coefficient (D) of the beads in the film after Eq. 4, and is modulated by the shear viscosity of the film.[25] Clearly, the SM and Cer samples studied displayed two different types of behavior, either showing high D values (low shear viscosity and thus LE phase) or low D values (high shear viscosity and thus a denser phase state) (Fig. 3 and Table 2). Therefore, results ~~for~~ from diffusion parameters rather than f~~or~~ from compressibility properties allowed to confirm that pure h-28:4 SM monolayers are in a LE state while pure h-28:4 Cer are in a denser (LC-like) phase state at 30 mN/m.

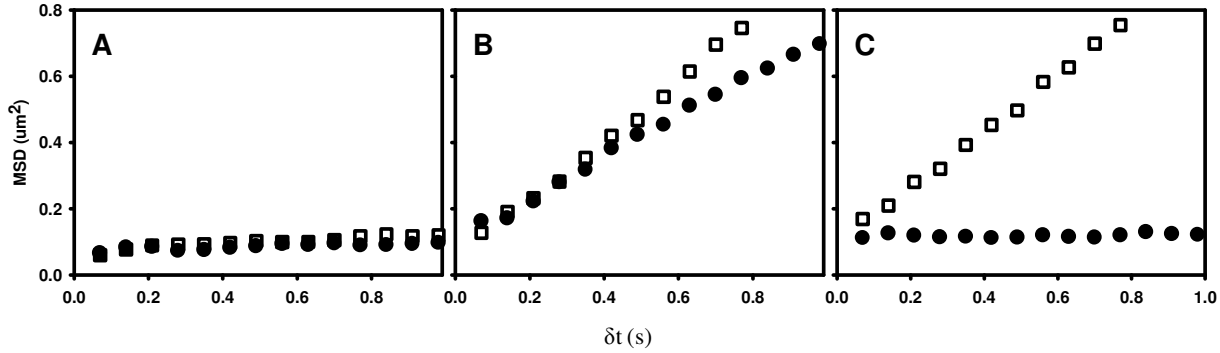

Figure 3.Tracking of single particles of latex beads on SM or Cer monolayers. Mean square displacement of 3 µm beads on sphingolipid monolayer of a representative experiment calculated at different time intervals (δt). The symbols represent monolayers of pure SM (squares) or pure Cer (circles) containing A) 16:0, B) 18:1 or C) h-28:4 acyl chains at 30 mN/m.

Monolayers of the two SMs that were in the LE state (18:1 SM and h-28:4 SM) had D values about ~20-fold higher than those of 16:0 SM (LE-LC phase coexistence) (Table 2), thereby falling in the same order as those reported for glycerophospholipids in the LE state (~1 $\mu m^2/s$).[32] Comparing SM and Cer, Catapano and coworkers reported a detailed rheology study of egg SM / egg Cer monolayers.[33] Using a system similar to ours, these authors found a 10-fold lower shear viscosity, and a 4-fold higher D value, for egg SM than for egg Cer when they are in a LC and a S state, respectively. In the present study we found little difference between D values of 16:0 SM (LE-LC) and 16:0 Cer (S state) (Table 2), even when 16:0 SM still contained a fraction of molecules in the LE state at the analyzed surface pressure[27] (perhaps isolated in discontinuous domains). This difference may arise because the diffusion properties in these samples were close to the detection limit of our method.

Comparatively, he D values for 18:1 SM (LE) were almost twice higher than for 18:1 Cer (LE) but~~and~~, surprisingly, were more than 100-fold higher for h-28:4 SM (LE) than for h-28:4 Cer (LC) (Table 2). The D value we obtained for 16:0 Cer was similar to that previously reported for egg Cer,[33] a lipid whose behavior has been described as a 2D

solid capable of undergoing plastic deformation.[34] It was thus remarkable that the h-28:4 Cermonolayer allowed an even more restricted diffusion than that allowed by 16:0 Cer.

The question of why, in contrast to h-28:4 SM, h-28:4 Cer shows an unusual behavior characterized by an easily compressible LC phase but with a highly restricted lateral diffusion is highly intriguing. We previously hypothesized that, considering the large MMA of VLCPUFA-containing Cers, their polar headgroup might be too small to prevent the bulky VLCPUFA from contacting the aqueous phase, and that the unsaturated portion of the acyl chains might be bent, highly disordered and partially hydrated.[20] This was supported by the notably large MMA and by the high ΔG_c obtained for h-28:4 Cer (26% higher than the energy required to compress a h-28:4 SM and 10-fold higher than to compress 16:0 Cer, see Table 2). This behavior may be ascribed to condensation of the acyl chains (measured as molecular area decrease after Eq. 7) in an extent that contributes to ΔG_c in 0.50 ± 0.01 kcal/mol (calculated as $-T.\Delta S_{cf}$). On the contrary, h-28:4 SM showed a lower ΔS_{cf} ascribable to area changes, which corresponds to 0.34 ± 0.01 kcal/mol ($-T.\Delta S_{cf}$). In section 3.1., this entropic decrease is proposed to be counteracted mainly by a release of water molecules from the hydration shell of the large phosphocoline group.

Table 2. Comparative analysis of physical parameters of SM and Cer monolayers at 30 mN/m

	Sphingomyelins			Ceramides		
N-linked fatty acid	16:0	18:1	h-28:4	16:0	18:1	h-28:4
MMA ($Å^2$/molec)	47 ± 1[a]	60 ± 1[a]	83 ± 1	41 ± 1[b]	50 ± 2[b]	58 ± 4[b]
Cs^{-1} (mN/m)	160 ± 3	106 ± 6	90 ± 9	433 ± 10	91 ± 6	74 ± 9
D (10^{-4}. $\mu m^2/s$)[c]	57 ± 10	1370 ± 80	1240 ± 130	40 ± 7	785 ± 60	11 ± 3
ΔG_c[a] (kcal/mol)[d]	0.35 ± 0.01	0.36 ± 0.01	0.57 ± 0.04	0.07 ± 0.01	0.30 ± 0.05	0.72 ± 0.02
ΔV (mV)	297 ± 14	199 ± 7	156 ± 5	513 ± 20	274 ± 6	248 ± 5
Phase state	LE-LC	LE	LE	S	LE	LC

[a] From [27]
[b] From [20]
[c] Calculated from 15-20 individual single particle tracking experiments after eq. 4
[d] Integrated compression isotherms from 1 to 35 mN/m after eq. S1.

Thus, different thermodynamic behavior correlated with differences in the rheological properties of the VLCPUFA-containing sphingolipids. In this regard, h-28:4 SM behaved as expected for an LE phase with relatively low Cs^{-1} and highly fluid behavior (high D). The bulky phosphocholine polar group of SM may prevent the interaction of the VLCPUFA with the aqueous subphase. By comparison, as suggested by a high loss of entropy upon compression, with negative ΔS_c, in h-28:4 Cer molecules a higher chain disorder and conformational freedom results in a soft-condensed phase, low Cs^{-1} values and high viscoelastic properties. This behavior resembles the one described for

polymer monolayers in a semidilute regime and good solvent conditions.[35] Such polymer films show relatively low compression modulus and low (gel-like) diffusional properties due to an interpenetrated network of the long chained structures, which leads to hindered motion resulting from entanglements of the fluid-likechains. .

3.3. Films prepared with mixtures of increasing SM / Cer ratios. We further studied the properties of h-28:4 SM/h-28:4 Cer mixed films in equilibrium conditions (monolayers formed by pre-mixed lipids) and in films generated by the action of sphingomyelinase (SMase) on pure SM monolayers in out-of equilibrium conditions (see section 3.4).[8,12]

In comparison with the pure components, pre-mixed SM / Cer monolayers showed compression isotherms with intermediate properties (Fig. 4A). Pure h-28:4 Cer underwent a LE $\rightarrow$ LC phase transition at 15 ± 1 mN/m at room temperature. This transition pressure increased as the monolayer was enriched in h-28:4 SM, indicating a stabilization of the LE state by a favorable mixing of the components (Fig. 4B-I).

As a general rule, when two or more components mix, the entropy of the system increases and the mixture is thermodynamically more stable than the pure components. Thus, the binary LE phase becomes more stable than the LC phase and predominates at higher pressures. This was demonstrated for 16:0 SM / 16:0 Cer mixtures, where 16:0 Cer mixes ideally with 16:0 SM-rich liquid-disordered membranes ($X_{Cer} < 0.4$) both in monolayer and bilayer systems.[36,37]

The excess free energy of mixing (ΔG_{exc}) represents the energy difference between the ΔG_c of a binary monolayer and the ΔG_c calculated for an ideal mixture.[22] In the present study, the ΔG_{exc} of SM / Cer mixtures showed positive values when the monolayers contained a mole fraction of Cer (X_{Cer}) ≥0.25 (Fig. 4B-II). This may be due to the prevalence of the LE phase. As accounted for by a larger area change, this phase provided higher entropy to the system over a wider pressure range than the ideal (non-interacting) behavior, and thus more energy was necessary to compress the film (see inset in Fig. 4A).

At 30mN/m, a linear behavior of the plot relating the average molecular dipolar moment ($\mu_\perp$) with the film composition (Fig. 4B-III) was observed. This indicates that each molecule was in an environment that is close to that expected for a pure component monolayer. This condition can be fulfilled either when ideal mixing or when a complete demixing of the components occurs.[22] This independent parameter represents the contribution of the molecular dipolar components perpendicular to the interface to the total surface potential of the film. Interestingly, the variation of MMA with the proportion of Cer did not show a linear relationship at all Cer concentrations, but showed a region of condensation at X_{Cer}≥0.50 (Fig. 4B-IV).

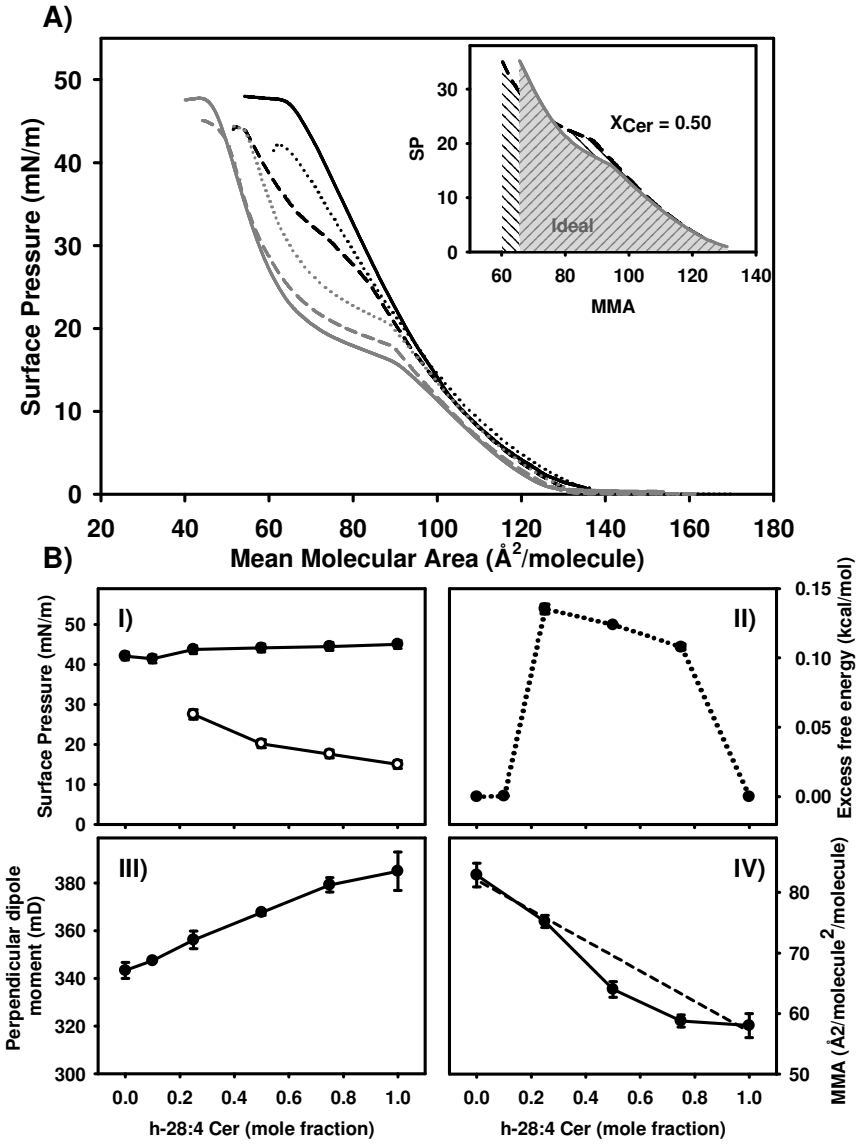

Figure 4.Compression isotherms of monolayers having different proportions of h-28:4 SM and h-28:4 Cer. A): The compression lines represent data from pure h-28:4 SM (black) and pure h-28:4 Cer (gray) monolayers, flanking data from mixed films, each containing 0.1 (dashed gray), 0.25 (dotted gray), 0.5 (dashed black), or 0.75 (dotted black) Cer / SM mole ratios, at 22C°. Each curve shows a representative experiment that differed in less than 2 Å^2/molecule and 2 mN/m from their replicas. B) The lower panels show, for the same SM / Cer binary mixtures: I) the phase diagram of the binary mixture, showing the LE $\rightarrow$ LC transition pressure (white circles) and the transition pressure to collapsed phase (black circles) (SEM values are within the size of the points); in II) the excess free energy of compression (ΔG_{exc}) of pure and binary monolayers, as calculated from the area under the compression curves from 1 to 35 mN/m. In III) the molecular dipole moment perpendicular to the interface ($\mu_{\perp}$); and in IV) the mean molecular area of the components in the mixed films at 30 mN/m are shown as a function of composition. The inset in (A) shows that the area under the experimental isotherm of the monolayer containing X_{Cer} = 0.5 (dashed black) is larger than the area (gray zone) under the ideal curve. The dashed line in (IV) represents the expected mixing behavior, should it be ideal.

BAM visualization of the binary SM / Cer films allowed analyzing the phase area distribution of the mixed monolayers (Fig. 5). At 30 mN/m, the mixed films showed a homogeneous LE phase up to $X_{Cer} \sim 0.25$. Rounded domains appeared al higher X_{Cer}, increasing until a very small fraction of LE phase remained in pure h-28:4 Cer monolayers. It may be hypothesized that a tie line is established between an LE phase containing $X^{LE}_{Cer} = 0.25$ and an LC phase of nearly pure h-28:4 Cer ($X^{LC}_{Cer} \sim 1$).

The lever rule determines that, for coexisting LE / LC phases, the surface area covered by each phase should be a function of the composition and of the molecular area of the components at the phase boundary, provided that the coexisting phases remain constant in composition along the tie line.[38] The BAM image analysis of monolayers having increasing proportions of Cer ($0.25 < X_{Cer} < 1.0$) gave results that suggested an LC phase coverage larger than that expected from the lever rule (Fig. 5B, see also section S2 in supplementary material). This coincided with the compositional range where a condensation of the MMA was observed (Fig. 4B-IV).

The results described so far indicated that h-28:4 SM was partially incorporated into the h-28:4Cer-enriched condensed domains in a fashion that depended on X_{Cer}. As the fraction of SM in such phase should decrease as X_{Cer} increased, the LC phase composition appears not to remain constant as imposed by the lever rule along the compositional axis at constant pressure. Therefore, the incorporation of SM into the Cer-enriched domains induced an isothermal LE $\rightarrow$ LC phase conversion of SM in the Cer- enriched environment, which explains the area condensation observed in Fig. 4B-IV. A similar observation was previously reported for 16:0 SM / 16:0 Cer mixed monolayers.[36] At low π values (< 15mN/m), pure 16:0 SM was in an LE state and pure 16:0 Cer was in the LC state. Then, a low solubility of 16:0 Cer in the LE phase was observed ($X^{LE}_{Cer} \sim 0.05$) and the composition of the LC phase showed a high content of SM ($X^{LC}_{Cer} \sim 0.4$). This was interpreted as a thermodynamically stable compositional point, a conclusion that was later supported in bilayers systems.[37]

A detailed study of the solubility of Cer species with different acyl-chain lengths in liposomes of 16:0 SM[39] demonstrated that the solubility of Cer into SM-enriched membranes is lower for the shorter 16:0 Cer ($X_{Cer} < 0.05$) than for the longer and unsaturated 24:1 Cer (up to $X_{Cer} = 0.1$). This gives support to the present results, as the miscibility of the even longer and unsaturated h-28:4 Cer in films of h-28:4 SM was even higher ($X_{Cer} \sim 0.25$).

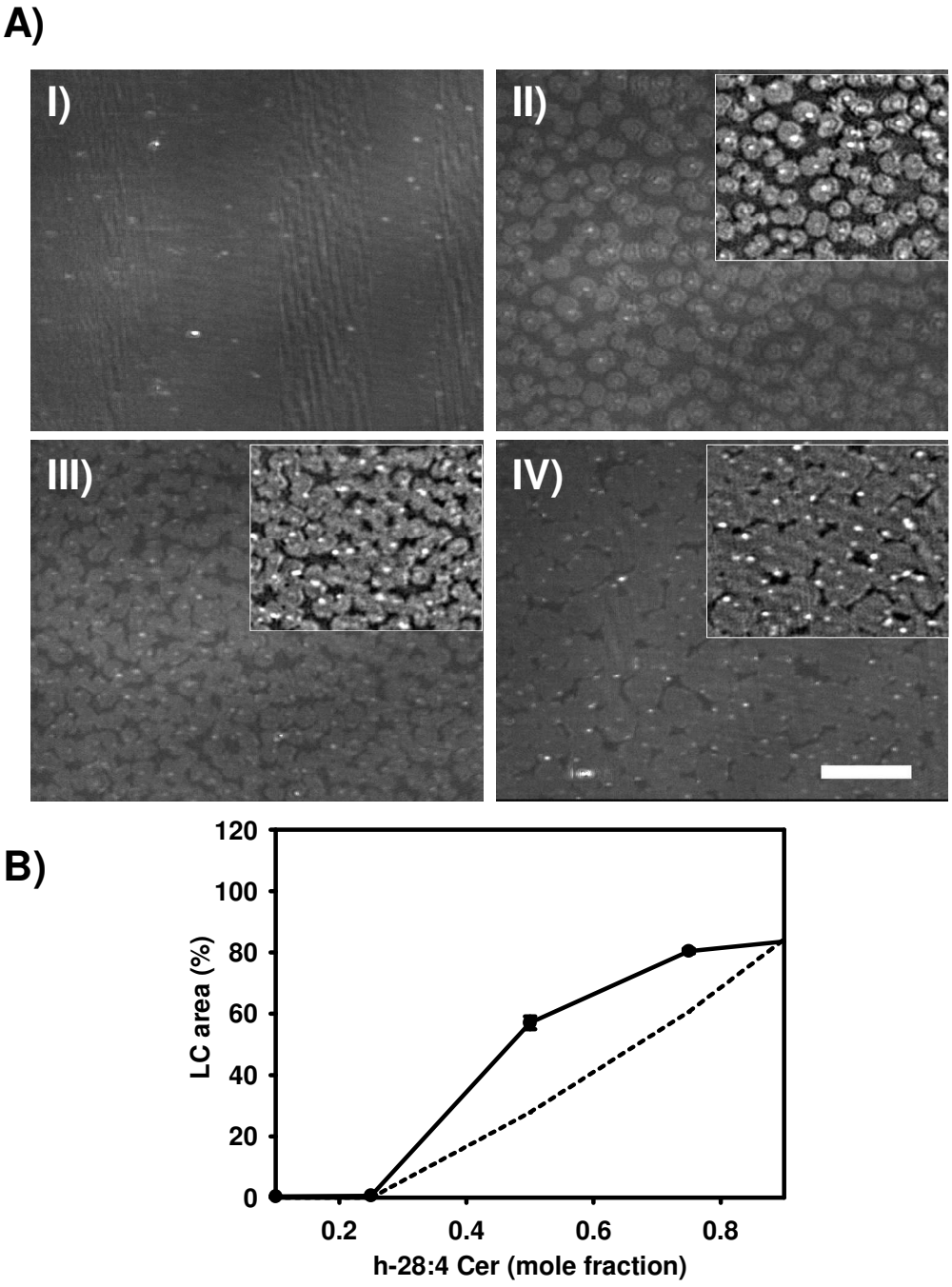

Figure 5.Binary h-28:4 SM and h-28:4 Cer phases coexisting in Langmuir monolayer. A) BAM images at 30 mN/m of mixed monolayers containing I) 0.25, II) 0.50, III) 0.75 (mole fraction) Cer in SM and IV) pure h-28:4 Cer. The insets show the same images enhanced by a bandpass filter. The bar in IV) represents 50 µm. B) Area percent occupied by the LC phase in mixed monolayers at 30 mN/m (symbols). The error bars are SEM from 4-10 pictures from two independent experiments. The dotted line represents the ideal area percent, according to the lever rule, that should be occupied by the LC phase if it was composed of pure h-28:4 Cer and if it was in equilibrium with an LE phase containing 0.25 mol% of Cer (see section 2.6).

3.4. Films of SM / Cer mixtures generated by SMase. Whereas the SMase used in this study has a high activity against pure 16:0 SM monolayers at low π values (3.4 ± 0.3 x10^{13} molec . min^{-1}. cm^{-2} at 10 mN/m), its activity approaches zero values above the LE $\rightarrow$ LC transition pressure.[8] Such a high sensitivity of this enzyme to the phase state of its substrate was also reported for bilayer systems.[10] Contrary to 16:0 SM monolayers, those of h-28:4 SM provided an LE film over the whole range of π, and SMase remained active against h-28:4 SM films at higher surface pressures (2.4 ± 0.3 x10^{13} molec. min^{-1}. cm^{-2} at 20 mN/m). In bilayers, evidence has been provided that VLCPUFA SMs have relatively low transition temperatures, and that they induce a decrease of the transition of DMPC in mixed vesicles.[13] On these bases, it was expected that the latter SMs would be good substrates for SMase, perhaps better than 16:0 SM.

However, the enzymatic activity was somewhat lower in the h-28:4 SM than in the 16:0 SM film. This may be a consequence of two factors; on one hand, it may be derived from a different surface density of the substrate, and on the other, there might be a preference of the enzyme for 16:0 SM over h-28:4 SM as substrate. Considering that *Bacillus cereus* SMase did not discriminate between 16:0 SM and 18:1 SM as substrates (not shown), and that there is a significant difference of MMA among substrates (see Fig. 2), which leads to differences in the substrate surface densities, we suggest that this was the main factor affecting the different activities. The films containing 16:0 SM at 10 mN/m had a surface density of 1.52 x 10^{14} molecules/cm^2, while those of h-28:4 SM at 20 mN/m contained 1.075 x 10^{14} molecules/cm^2 (a reduction of ~30%). This coincided with the fact that SMase is highly sensitive to substrate density in a Michaelian way.[8]

The BAM images in Fig. 6 showed that the SM $\rightarrow$ Cer hydrolytic process occurs with the nucleation (and growth) of Cer-enriched condensed domains that appeared as star-like shapes for 16:0 SM / Cer but as rounded shapes for h-28:4 SM / Cer. The star-like shape may have developed from intra-domain dipolar repulsion, due to the large difference in the overall surface potential of the SM- and Cer-enriched phases.[8] The surface topography obtained enzymatically from h-28:4 SM films at long reaction times, i.e., once the SMase action had concluded, led to the formation of worm-like domains that were produced by fusion of the rounded domains. Such change was not observed in the pre-mixed h-28:4 SM / Cer films. This difference could be a consequence of a far-from-equilibrium nucleation and domain growth process caused by SMase action, as it has been also previously described for 16:0 SM / Cer.[8] In the latter case, domain shape annealing in the order of tenths of minutes was attributed to a slow rate of diffusion of the SM component into the LC phase.

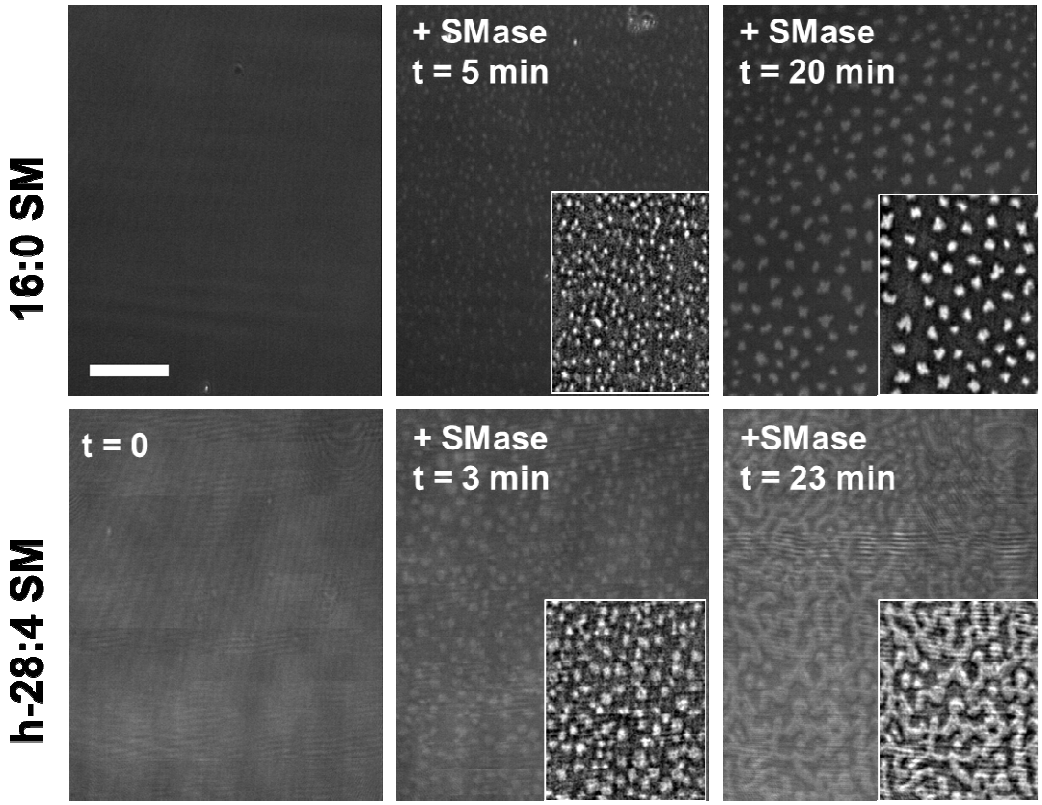

Figure 6. SM / Cer films generated by sphingomyelinase (SMase) activity. Comparison of BAM images from initially pure 16:0 SM at 10 mN/m and h-28:4 SM at 20mN/m, before (t=0), and at different times after SMase treatment. The insets show the same images enhanced by a bandpass filter. The bar size represents 50 µm.

The surface potential difference between a pure h-28:4 SM and a pure h-28:4Cer monolayer was relatively small (~90mV) if compared to that of the 16:0 SM / 16:0 Cer pair (> 200 mV, see Table 2). Thus, linear tension predominated over intra-domain repulsion, favoring rounded domain structures with a low boundary/area relationship in the former compared with the latter (Fig. 6).

The difference in dipolar properties of the coexistent phases is also a factor of importance for the establishment of inter-domain structures. The enzymatically generated 16:0 SM / 16:0 Cer interfaces show a long range domain ordering into a hexagonal lattice because the inter-domain repulsion overcomes the thermal energy.[8] The inter-domain repulsion should be relatively lower in h-28:4 SM / h-28:4Cer than in 16:0 SM / 16:0 Cer films. This factor, in addition to an enhanced dynamics of the monolayer in out-of-equilibrium conditions (i. e. during SMase action), favors domain fusion leading to formation of worm-like domains (Fig. 6).

As a consequence, the h-28:4 SM / h-28:4 Cer films showed several similarities with the shorter 16:0 SM/16:0 Cer pair, but allowed SMase action and formation of Cer-enriched domains at higher π (closer to the bilayer average pressure). The h-28:4 SM/h-28:4 Cer films also incorporated a larger amount of Cer into the LE phase than did the 16:0 SM/16:0 Cer monolayers, and promoted a different surface texture as a consequence of lower dipolar repulsion.

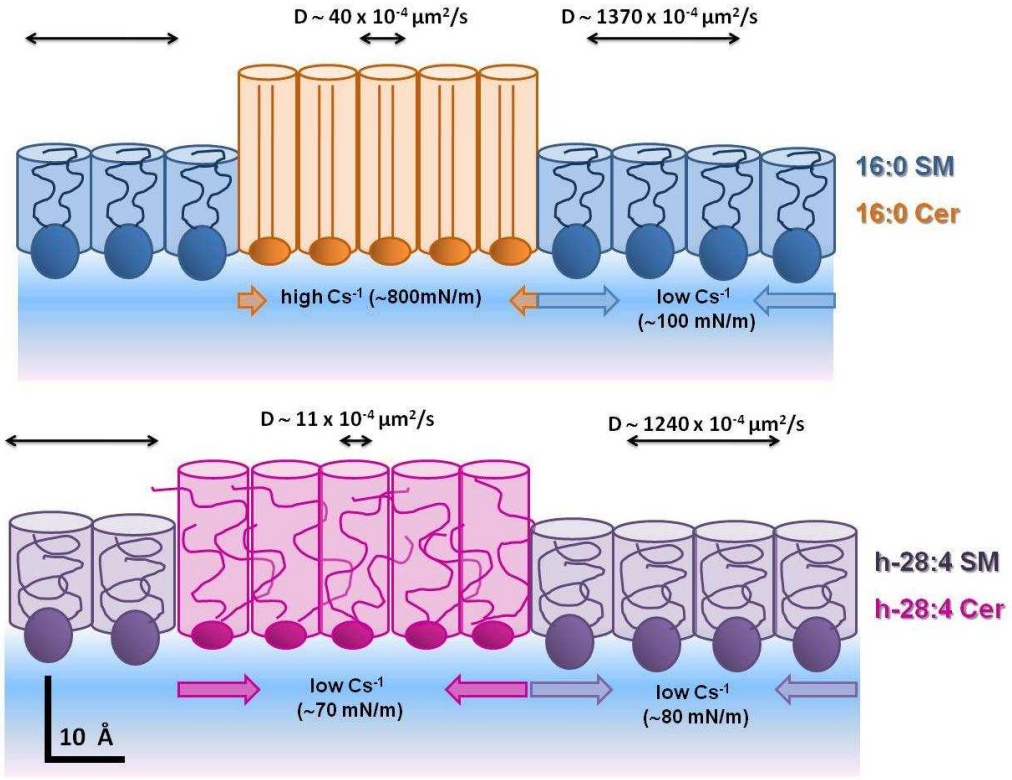

Fig. 7. Schematic representation of SM- and Cer-enriched films with phase coexistence. The cylindrical objects represent an in scale dimension of the volume occupied by 16:0 SM (blue), 16:0 Cer (orange), h-28:4 SM (violet) and h-28:4 Cer (magenta). The straight lines within the orange cylindrical objects represent the two hydrocarbon chains in a straight conformation of the solid 16:0 Cer -enriched phase, while the curved lines within the magenta cylinder represent the entangled chains of the soft liquid-condensed phase enriched in h-28:4 Cer. The SM-enriched phases are represented in a liquid-expanded state (at 10mN/m for 16:0 SM and at 30mN/m for h-28:4 SM). The arrows above each phase represent the lateral mobility of the phase components according to single particle tracking experiments and the color arrows below each phase represent the compressibility properties of the film. The D and Cs^{-1} values ~~are~~ were taken from Table 2.

One of the original intriguing questions which moved us to start studying this particular family of sphingomyelins containing VLCPUFA was how such unusually long acyl chains accommodate in a regularly sized membrane, i.e., whether these SMs form a thicker film, laterally separated from other components, or whether the chains adapt their length (e.g., by bending) to the normal membrane thickness. Our results show that VLCPUFA-containing SM in the LE state (as they are at physiological temperatures) form films with thickness similar as those of shorter SMs in the same phase state (Fig. 7), and that they share many of their common properties (Fig. 7 and Table 2). This supports the view that the VLCPUFA-SMs that occur in the spermatozoa head membrane may freely diffuse, mix and interact with other membrane components as would a common glycerophospholipid, i.e. one having a saturated acyl chain at sn-1 and a polyunsaturated acyl chain at the sn-2 of the glycerol backbone.

When SM containing VLCPUFA are enzymatically converted to Cer, the latter laterally segregate into thicker domains with hindered lateral diffusion of its components, but, different to shorter and saturated Cers, they show a soft compressible behavior (Fig. 7). This unusual feature, which reminds the properties of polymer films with entanglement of their chains, had not been previously reported for a film from a naturally occurring lipid, as far as we know. Whether this is a behavior common to VLCPUFA containing lipids in the LC state or it is a particular property of VLCPUFA-containing ceramides remains to be investigated.

4. CONCLUSIONS

Taken together, the different approaches used here indicate that the films of VLCPUFA-containing SMs are quite disordered, with large areas per molecule and low film thickness. This implies rather weaker intermolecular interactions compared to those occurring between SMs with relatively shorter and straight-chain saturated fatty acids, as is the case of the better-known 16:0 SM. The VLCPUFA 32:5, 28:4, and 30:5 do have a saturated hydrocarbon chain segment with 14, 13, and 12 methylene groups, respectively, from the carboxyl group involved in the amide bond to the first of the series of methylene-interrupted *cis* double bonds. This segment of the molecules would be the one interacting under pressure, explaining that VLCPUFA-SM properties in monolayers and bilayers in general tended to be more fluid and more disordered than their better known counterparts with shorted acyl chains.

Upon cooling, only the longest n-32:5 SM and h-32:5 SM showed an LE → LC phase transition in monolayers and also were the only ones to show a transition temperature, close to room temperature, in bilayers[13] The differences observed between n-V SM and their corresponding h-V SM species were consistent with those previously seen in their chain-matched Cers,[20] the hydroxyl group at C2 of the N-acyl chains in both cases imposing a stronger attraction among molecules.

The hydrophobic chain mismatch between the (C18) length of sphingosine and that of the N-acyl chain in the sperm-specific sphingolipids having VLCPUFA is another feature that distinguishes them from better-known SM and Cer species and in part explains the present observations. In previous work studying the behavior in Langmuir monolayers of Cers with saturated fatty acids varying in chain length (C10, C12, C14 and C16),[17] the film thickness and the surface dipole moment of the condensed state increased with the N-acyl chain length. However, several features were observed in the surface electrostatics, topography, and thickness of the films in Cers with shorter fatty acids that were ascribed to the asymmetry established between the (C18) length of sphingosine and that of the acyl chain. Such results supported the view that a bending of the hydrocarbon segment of the *sphingosine* moiety that exceeds the length of the fatty acyl chain probably occurs in the LC state, thus alleviating the hydrophobic chain mismatch while keeping as much as possible the hydrophobic interactions.

In the case of SMs and Cers containing 28-32 carbon-VLCPUFA, the opposite mismatch occurs, as the N-linked acyl chain length exceeds in several carbon atoms the C18 length of sphingosine. In the present case the fatty acid should be the one to bend over its own length in the air phase to interact with the “shorter” sphingosine

chain, as supported by the low value of the semiempirical thickness of the films made of VLCPUFA containing SM and also of Cer[20] species.

The present results show that VLCPUFA-containing SMs have structural and rheological properties that are not too far from those of shorter SMs and thereby could be accommodated into planar lipid monolayers. By contrast, the corresponding VLCPUFA-Cers display atypical rheological properties when organized in a planar monolayer structure, characterized by the presence of a highly compressible LC phase (polymer-like behavior) likely due to a highly disordered conformation of the partially hydrated fatty acyl moiety. These observations, together with the finding that the process of enzymatic generation of Cer from VLCPUFA-SM results in the nucleation (and growth) of Cer-enriched condensed domains at high surface pressures, may be related to the function of Cer in spermatozoa.

The Cer species produced after the acrosomal reaction (AR) in rat spermatozoa are formed *in situ* by a form of SMase that uses endogenous SMs as substrates. A Mg^{2+}-dependent neutral sphingomyelinase has been characterized in the plasma membrane of rat spermatozoa [40] that could, in part, be responsible for the irreversible SM → Cer conversion observed after completion of the AR. These Cer species are not hydrolyzed further and thus remain associated with the gametes.

Fusion events take place on the own surface of the sperm head during the AR. These are believed to lead to the creation of several points of membrane fusion between the outer leaflet of the acrosomal membrane and the inner leaflet of the plasma membrane, thereby forming discontinuities on the sperm head surface that increase the membrane permeability to allow the release of the acrosomal contents[41,42]. As sperm SM with VLCPUFA are mostly located in the sperm head[6], also should the VLCPUFA-Cer created after completion of this reaction. Taking into account that Cers favor lipid structures with high curvature[43,44] and that sperm undergo an important restructuring of its membrane after the AR, the generated Cer could play their role in the acquisition of sperm fusogenic capacity. The generation of Cer from SM could play a functional role in promoting these life-essential membrane changes.

AUTHOR INFORMATION

Corresponding Author
*Telephone: +54 351 4334168. Fax: +54 351 4334074. E-mail: lfanani@fcq.unc.edu.ar.

ACKNOWLEDGMENTS

This work was supported by the Consejo Nacional de Investigaciones Científicas y Técnicas (CONICET), Agencia Nacional de Promoción Científica y Tecnológica (ANPCyT), and the General Secretariats of Science and Technology of the Universidad Nacional de Córdoba (UNC) y Universidad Naconal del Sur (UNS), Argentina.
Supporting Information Available. This information is available free of charge via the Internet at http://pubs.acs.org.

ABBREVIATIONS

Cer, ceramide; Chol, cholesterol; PC, phosphatidylcholine; SM, sphingomyelin; SMase, sphingomyelinase; VLCPUFA, very long chain polyunsaturated fatty acids, with h-V and n-V indicating 2-hydroxy VLCPUFA and nonhydroxy VLCPUFA, respectively; μ, dipole moment perpendicular to the interface; ΔG_c, Gibbs free energy change of compression; ΔG_{exc}, excess free energy of compression; ΔS_c, entropy change of compression; ΔV, surface potential; π, surface pressure; π_s, interaction pressure; BAM, Brewster angle microscopy; Cs^{-1}, compressibility modulus; D, diffusion coefficient; LC, liquid-condensed; LE, liquid-expanded; MMA, mean molecular area; MSD, mean square displacement; S, solid phase; *Th*, semi-empirical film thickness; *V*, semi-empirical molecular volume; X^{LC}_{Cer}, mole fraction of ceramide in the liquid-condensed phase; X^{LE}_{Cer}, mole fraction of ceramide in the liquid-expanded phase.

References

(1) *Poulos, A.; Sharp, P.; Johnson, D.; White, I.; Fellenberg, A. The occurrence of polyenoic fatty acids with greater than 22 carbon atoms in mammalian spermatozoa. Biochem. J.* ***1986,*** *240 (3), 891-895.*

(2) *Poulos, A.; Johnson, D. W.; Beckman, K.; White, I. G.; Easton, C. Occurrence of unusual molecular species of sphingomyelin containing 28-34-carbon polyenoic fatty acids in ram spermatozoa. Biochem. J.* ***1987,*** *248 (3), 961-964.*

(3) *Sandhoff, R. Very long chain sphingolipids: tissue expression, function and synthesis. FEBS Lett.* ***2010,*** *584 (9), 1907-1913.*

(4) *Robinson, B. S.; Johnson, D. W.; Poulos, A. Novel molecular species of sphingomyelin containing 2-hydroxylated polyenoic very-long-chain fatty acids in mammalian testes and spermatozoa. J. Biol. Chem.* ***1992,*** *267 (3), 1746-1751.*

(5) *Zanetti, S. R.; de Los Angeles, M. M.; Rensetti, D. E.; Fornes, M. W.; Aveldano, M. I. Ceramides with 2-hydroxylated, very long-chain polyenoic fatty acids in rodents: From testis to fertilization-competent spermatozoa. Biochimie* ***2010,*** *92 (12), 1778-1786.*

(6) *Oresti, G. M.; Luquez, J. M.; Furland, N. E.; Aveldano, M. I. Uneven distribution of ceramides, sphingomyelins and glycerophospholipids between heads and tails of rat spermatozoa. Lipids* ***2011,*** *46 (12), 1081-1090.*

(7) *Zanetti, S. R.; Monclus, M. L.; Rensetti, D. E.; Fornes, M. W.; Aveldano, M. I. Differential involvement of rat sperm choline glycerophospholipids and sphingomyelin in capacitation and the acrosomal reaction. Biochimie* ***2010,*** *92 (12), 1886-1894.*

(8) *Fanani, M. L.; Hartel, S.; Maggio, B.; De, T. L.; Jara, J.; Olmos, F.; Oliveira, R. G. The action of sphingomyelinase in lipid monolayers as revealed by microscopic image analysis. Biochim. Biophys Acta* ***2010,*** *1798, 1309-1323.*

(9) *Holopainen, J. M.; Subramanian, M.; Kinnunen, P. K. Sphingomyelinase induces lipid microdomain formation in a fluid phosphatidylcholine/sphingomyelin membrane. Biochemistry* ***1998,*** *37 (50), 17562-17570.*

(10) *Ruiz-Arguello, M. B.; Veiga, M. P.; Arrondo, J. L.; Goni, F. M.; Alonso, A. Sphingomyelinase cleavage of sphingomyelin in pure and mixed lipid membranes. Influence of the physical state of the sphingolipid. Chem Phys Lipids* ***2002,*** *114 (1), 11-20.*

(11) *Boulgaropoulos, B.; Amenitsch, H.; Laggner, P.; Pabst, G. Implication of sphingomyelin/ceramide molar ratio on the biological activity of sphingomyelinase. Biophys. J.* ***2010,*** *99 (2), 499-506.*

(12) *Chao, L.; Gast, A. P.; Hatton, T. A.; Jensen, K. F. Sphingomyelinase-Induced Phase Transformations: Causing Morphology Switches and Multiple-Time-Domain Ceramide Generation in Model Raft Membranes. Langmuir* ***2010,*** *26 (1), 344-356.*

(13) *Peñalva, D. A.; Furland, N. E.; Lopez, G. H.; Aveldaño, M. I.; Antollini, S. S. Unique thermal behavior of sphingomyelin species with nonhydroxy and 2-hydroxy very-long-chain (C28-C32) polyunsaturated fatty acids. J. Lipid Res.* ***2013,*** *54 (8), 2225-2235.*

(14) *Ramstedt, B.; Slotte, J. P. Sphingolipids and the formation of sterol-enriched ordered membrane domains. Biochim Biophys Acta* ***2006,*** *1758 (12), 1945-56.*

(15) *Li, X. M.; Momsen, M. M.; Brockman, H. L.; Brown, R. E. Sterol structure and sphingomyelin acyl chain length modulate lateral packing elasticity and detergent solubility in model membranes. Biophys. J.* ***2003,*** *85 (6), 3788-3801.*

(16) *Jaikishan, S.; Slotte, J. P. Effect of hydrophobic mismatch and interdigitation on sterol/sphingomyelin interaction in ternary bilayer membranes. Biochim Biophys Acta* ***2011,*** *1808 (7), 1940-1945.*

(17) *Dupuy, F.; Fanani, M. L.; Maggio, B. Ceramide N-Acyl Chain Length: A Determinant of Bidimensional Transitions, Condensed Domain Morphology, and Interfacial Thickness. Langmuir* ***2011,*** *27 (7), 3783-3791.*

(18) *Brockman, H. L.; Momsen, M. M.; Brown, R. E.; He, L.; Chun, J.; Byun, H. S.; Bittman, R. The 4,5-double bond of ceramide regulates its dipole potential, elastic properties, and packing behavior. Biophys. J.* ***2004,*** *87 (3), 1722-1731.*

(19) *Goni, F. M.; Alonso, A. Biophysics of sphingolipids I. Membrane properties of sphingosine, ceramides and other simple sphingolipids. Biochim Biophys Acta* ***2006,*** *1758 (12), 1902-1921.*

(20) *Peñalva, D. A.; Oresti, G. M.; Dupuy, F.; Antollini, S. S.; Maggio, B.; Aveldaño, M. I.; Fanani, M. L. Atypical surface behavior of ceramides with nonhydroxy and 2-hydroxy very long-chain (C28-C32) PUFAs. Biochim Biophys Acta* ***2013****, 1838, 731-738.*

(21) *Brown, R. E.; Brockman, H. L. Using monomolecular films to characterize lipid lateral interactions. Methods Mol. Biol.* ***2007,*** *398, 41-58.*

(22) *Gaines, G. L. Insoluble monolayers at liquid-gas interfaces.; Interscience Publishers: New York, 1966.*

(23) *Davies, J. T.; Rideal, E. K. Interfacial Phenomena; Academic Press: NY, 1963.pp. 217-281.*

(24) *Jungner, M.; Ohvo, H.; Slotte, J. P. Interfacial regulation of bacterial sphingomyelinase activity. Biochim Biophys Acta* ***1997,*** *1344, 230-240.*

(25) *Wilke, N.; Vega, M. F.; Maggio, B. Rheological Properties of a Two Phase Lipid Monolayer at the Air/Water Interface: Effect of the Composition of the Mixture. Langmuir* ***2010****.*

(26) *Lheveder, C.; Meunier, J.; Henon, S. Brewster Angle Microscopy. In Physical Chemistry of Biological Interfaces, Baszkin, A., Norde, W., Eds.; Marcel Dekker, Inc: NY, 2000.*

(27) *Li, X. M.; Smaby, J. M.; Momsen, M. M.; Brockman, H. L.; Brown, R. E. Sphingomyelin interfacial behavior: the impact of changing acyl chain composition. Biophys. J.* ***2000,*** *78 (4), 1921-1931.*

(28) *Fidelio, G. D.; Maggio, B.; Cumar, F. A. Molecular parameters and physical state of neutral glycosphingolipids and gangliosides in monolayers at different temperatures. Biochim Biophys Acta* ***1986,*** *854 (2), 231-9.*

(29) *Israelachvili, J. N.; Marcelja, S.; Horn, R. G. Physical principles of membrane organization. Q Rev Biophys* ***1980,*** *13 (2), 121-200.*

(30) Maggio, B. Geometric and thermodynamic restrictions for the self-assembly of glycosphingolipid-phospholipid systems. Biochim Biophys Acta **1985,** 815 (2), 245-58.

(31) Israelachvili, J. N. Intermoecular and surface forces; 2 nd ed.; Academic Press: London, 1992.

(32) Forstner, M. B.; Kas, J.; Martin, D. Single Lipid diffusion in Langmuir Monolayers. Langmuir **2001,** 17 (3), 567-570.

(33) Catapano, E. R.; Arriaga, L. R.; Espinosa, G.; Monroy, F.; Langevin, D.; Lopez-Montero, I. Solid character of membrane ceramides: a surface rheology study of their mixtures with sphingomyelin. Biophys J. **2011,** 101 (11), 2721-2730.

(34) Lopez-Montero, I.; Catapano, E. R.; Espinosa, G.; Arriaga, L. R.; Langevin, D.; Monroy, F. Shear and compression rheology of Langmuir monolayers of natural ceramides: solid character and plasticity. Langmuir **2013,** 29 (22), 6634-6644.

(35) Martin, A. M. Dynamics of Interfacial systems; (PhD Thesis) ed.; Universidad Computense de Madrid, Facultad de Ciencias Químicas: 2010.

(36) Busto, J. V.; Fanani, M. L.; De, T. L.; Sot, J.; Maggio, B.; Goni, F. M.; Alonso, A. Coexistence of immiscible mixtures of palmitoylsphingomyelin and palmitoylceramide in monolayers and bilayers. Biophys J **2009,** 97 (10), 2717-2726.

(37) Leung, S. S.; Busto, J. V.; Keyvanloo, A.; Goni, F. M.; Thewalt, J. Insights into sphingolipid miscibility: separate observation of sphingomyelin and ceramide N-acyl chain melting. Biophys J. **2012,** 103 (12), 2465-2474.

(38) Fidorra, M.; Garcia, A.; Ipsen, J. H.; Hartel, S.; Bagatolli, L. A. Lipid domains in giant unilamellar vesicles and their correspondence with equilibrium thermodynamic phases: a quantitative fluorescence microscopy imaging approach. Biochim. Biophys Acta **2009,** 1788 (10), 2142-2149.

(39) Westerlund, B.; Grandell, P. M.; Isaksson, Y. J.; Slotte, J. P. Ceramide acyl chain length markedly influences miscibility with palmitoyl sphingomyelin in bilayer membranes. Eur. Biophys J. **2010,** 39 (8), 1117-1128.

(40) Hinkovska, V. T.; Petkova, D. H.; Koumanov, K. A neutral sphingomyelinase in spermatozoal plasma membranes. Biochem Cell Biol **1987,** 65 (6), 525-528.

(41) Nolan, J. P.; Hammerstedt, R. H. Regulation of membrane stability and the acrosome reaction in mammalian sperm. FASEB J **1997,** 11 (8), 670-682.

(42) Flesch, F. M.; Gadella, B. M. Dynamics of the mammalian sperm plasma membrane in the process of fertilization. Biochim Biophys Acta **2000,** 1469 (3), 197-235.

(43) Holopainen, J. M.; Angelova, M. I.; Kinnunen, P. K. Vectorial budding of vesicles by asymmetrical enzymatic formation of ceramide in giant liposomes. Biophys. J. **2000,** 78 (2), 830-838.

(44) Goni, F. M.; Contreras, F. X.; Montes, L. R.; Sot, J.; Alonso, A. Biophysics (and sociology) of ceramides. Biochem Soc Symp **2005,** (72), 177-188.

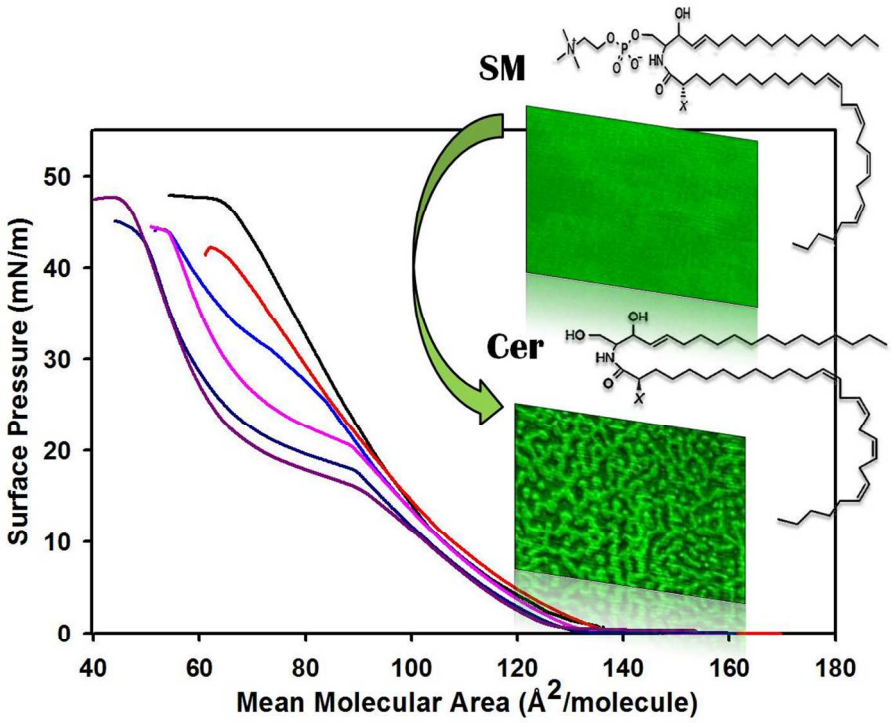

450x338mm (72 x 72 DPI)